

Article

Experimental Determination of CO₂ Diffusion Coefficient in a Brine-Saturated Core Simulating Reservoir Condition

Zerong Li, Lei Yuan, Guodong Sun, Junchen Lv and Yi Zhang * 

Key Laboratory of Ocean Energy Utilization and Energy Conservation Ministry of Education, School of Energy and Power Engineering, Dalian University of Technology, Dalian 116024, China; 732398470@mail.dlut.edu.cn (Z.L.); yuanlei@mail.dlut.edu.cn (L.Y.); sgd@mail.dlut.edu.cn (G.S.); lvjunchenzzz@mail.dlut.edu.cn (J.L.)

* Correspondence: Zhangyi80@dlut.edu.cn

Abstract: CO₂ diffusion coefficient plays a crucial part in saline aquifers for the CO₂ storage and the safety of long-term sequestration. Therefore, it is particularly important to measure the diffusion coefficient accurately. As far as we know, there are currently no CO₂ brine diffusion data in real cores under reservoir temperature and pressure conditions. In this paper, a study on the CO₂ diffusion coefficient diffused in a brine-saturated Berea core along the radial direction was conducted at temperatures of 313.15 K to 373.15 K and pressures of 8 MPa to 30 MPa. On account of the experimental results, the effect of permeability, NaCl concentration, temperature and pressure on the CO₂ diffusivity is analyzed. The results in this study indicate that the diffusion coefficient increases with increasing permeability, pressure and temperature and decreases with increasing NaCl concentration. However, the relationship between pressure and the diffusion coefficient is not linear. As the pressure gradually increases, the effect of pressure will become weak. In addition, an empirical correlation of the relationship between temperature–pressure and the CO₂ diffusion coefficient could be obtained based on the experimental data. The data in this paper fill the blank on the study of the CO₂ diffusivity in brine under reservoir conditions, which has positive significance for the study of supercritical CO₂ diffusion in a brine-saturated core.

Keywords: CO₂; diffusion coefficient; CO₂ geological storage; brine



Citation: Li, Z.; Yuan, L.; Sun, G.; Lv, J.; Zhang, Y. Experimental Determination of CO₂ Diffusion Coefficient in a Brine-Saturated Core Simulating Reservoir Condition. *Energies* **2021**, *14*, 540. <https://doi.org/10.3390/en14030540>

Academic Editors: Andrea De Pascale and Maria Alessandra Ancona
Received: 23 December 2020
Accepted: 19 January 2021
Published: 21 January 2021

Publisher's Note: MDPI stays neutral with regard to jurisdictional claims in published maps and institutional affiliations.



Copyright: © 2021 by the authors. Licensee MDPI, Basel, Switzerland. This article is an open access article distributed under the terms and conditions of the Creative Commons Attribution (CC BY) license (<https://creativecommons.org/licenses/by/4.0/>).

1. Introduction

It is widely believed that the main cause of the rise in global average temperature in the 20th century was greenhouse gas emissions caused by industrial activities [1–3]. CO₂ is the largest contributor to the greenhouse effect. Therefore, a lot of technologies have been proposed to reduce CO₂ emissions [4–7]. One of the technologies with a great development prospect is carbon capture and storage (CCS). It can reduce CO₂ concentration in the atmosphere and minimize the impact of human activity on the climate [8–13]. Saline aquifers have a well-developed trap structure, so they have become significant CO₂ storage reservoirs [14–17]. The diffusion coefficient of CO₂ determines the mass transfer rate [18]. Therefore, the CO₂ diffusion coefficient is of great significance for risk assessment and long-term storage in saline aquifer storage [19–21]. Accurate measurement of diffusion coefficient is of significant reference value for the sequestration of saline aquifers. Since 1930, the pressure volume temperature (PVT) method was mostly used to study CO₂ diffusion process [22–25]. It is common to discuss diffusion process by combining the PVT method with the pressure decay method. The constant volume PVT cell was used as the diffusion cell. The pressure-time distribution curve was obtained by measuring the pressure change in the diffusion cell in real time, and then the diffusion coefficient could be predicted according to the mathematical model [26]. The CO₂ diffusivity in the saline aquifer is closely relevant to the ambient temperature and pressure conditions. Some scholars have studied the CO₂ diffusion in pure water, but the experimental conditions in these studies

are far from the actual reservoir conditions. For instance, Tang and Himmelblau [27] used a large liquid-jet method to study the diffusion process of CO₂ in water at room temperature. Tamimi et al. [28] used a wetted-sphere absorption apparatus to discuss the CO₂ diffusion process in a temperature range of 293.15–368.15 K. Hirai et al. [29] reported CO₂ diffusion coefficients using laser-induced fluorescence in pure water at 286.15 K and at 9.40 MPa to 39.20 MPa.

So far, there are few literatures on measuring the CO₂ diffusion coefficient under reservoir conditions. Wang et al. [30] obtained the CO₂ diffusion coefficient in NaCl solution at the pressure of 1.52–5.18 MPa. Azin et al. [31] studied the CO₂ diffusion process in brine at the pressure of 5.90–6.90 MPa and the temperature of 305.15–323.15 K. Zarghami et al. [32] reported the influence of concentration on CO₂ diffusion process at pressure up to 17.45 MPa and temperature up to 341.15 K. Z. Shi et al. [33] measured the diffusion coefficient of CO₂ in brine with porous media using pressure decay method. The temperature and pressure conditions were 323.15 K and 6 MPa. Table 1 lists a summary of the CO₂ diffusion coefficient in pure water or brine reported in the literature.

Table 1. CO₂ diffusion coefficient in brine or pure water from the literature.

Source	Solution	Method	Porous Media	Temperature, K	Pressure, MPa	Diffusivity, 10 ⁻⁹ m ² /s
Azin [31]	Brine	Pressure decay method	/	305.15–323.15	5.90–6.90	3.52–6.16
Raad [34]	Brine	Pressure decay method	/	303.15–313.15	5.88–6.27	0.6–23
Renner [26]	Brine	Pressure decay method	/	311.15	1.54–5.83	3.07–6.86
Chaodong Yang [4]	Brine	Pressure decay method	/	300.15–331.15	2.60–7.50	170.7–269.8
Wang [35]	Brine	Pressure decay method	/	311.15	1.52–5.18	2.925–4.827
Zarghami [32]	Brine	Pressure decay method	/	323.15–348.15	17.45	6.5–8.2
Zhang [36]	Brine	Pressure decay method	/	298.15	1.17	1.5–1.91
Z. Shi [33]	Brine	Pressure decay method	Beads, quartz	323.15	6.00	1.25–82
Rasoul Nazari Moghaddam [37]	Brine	Pressure decay method	Sand	310.15	3.44	0.825–94.6
Belgodere [38]	Pure water	situ Raman spectroscopic measurement	Porous media	294.15	4.00	1.71
Cadogan [39]	Pure water	Taylor dispersion method	/	298.15–423.15	15.00–45.00	2.233–12.21
Farajzadeh [40]	Pure water	Pressure decay method	/	298.15–303.15	0.80–5.00	2.75–245
Frank [41]	Pure water	Taylor–Aris dispersion method	/	298.15–328.15	0.10	1.97–3.67
Hirai [29]	Pure water	laser-induced fluorescence	/	286.15	9.40–39.20	1–1.5
Lu [42]	Pure water	situ Raman spectroscopic measurement	/	268.15–473.15	20.00	0.7–1.6
Sell [43]	Pure water	Microfluidic method	/	299.15	0.50–5.00	1.86
Tamimi [27]	Pure water	liquid-jet method	/	293.15–368.15	0.10	2.11
Wang [35]	Pure water	Pressure decay method	/	318.15	3.43–8.02	233.6–251.34

It can be observed intuitively from Table 1 that the diffusivity values vary greatly in different studies. Experimental conditions are inconsistent with actual reservoir conditions, while experimental data for porous media under high temperature and pressure are scarce.

In this study, the influence of pressure, temperature, porous media permeability and salt concentration on CO₂ diffusion in brine were analyzed. Experimentally, the CO₂ diffusion coefficients in a brine-saturated Berea core under 33 different conditions were measured. The pressure and temperature range covered from 8 MPa to 30 MPa and 333.15 K to 373.15 K, respectively. The conditions in this study simulate the actual environment well. In the experiment, the CO₂ diffusion direction is radial diffusion instead of axial diffusion, which makes the experimental results more credible [8]. The empirical formula

of the CO₂ diffusion coefficient in a brine saturated core based on pressure-temperature was established. The principal goal of this study is to calculate the CO₂ diffusion coefficient and its affecting factors in cores saturated with brine. This study will provide exhaustive experimental data for CO₂ transport in consolidated porous media in saline aquifers.

2. Calculation Model

2.1. Physical Model of the Diffusion Experiment

Figure 1 shows the experimental diffusion model. H is the diameter of the reactor; r_0 is the core radius. The ends of the Berea core are sealed with resin to ensure that CO₂ could only diffuse into the brine-saturated core along the transverse direction. The s of the core is employed to calculate the diffusion coefficient. It can provide a greater contact surface, and more gases are used in the experiment. Thus, the results are more reliable.

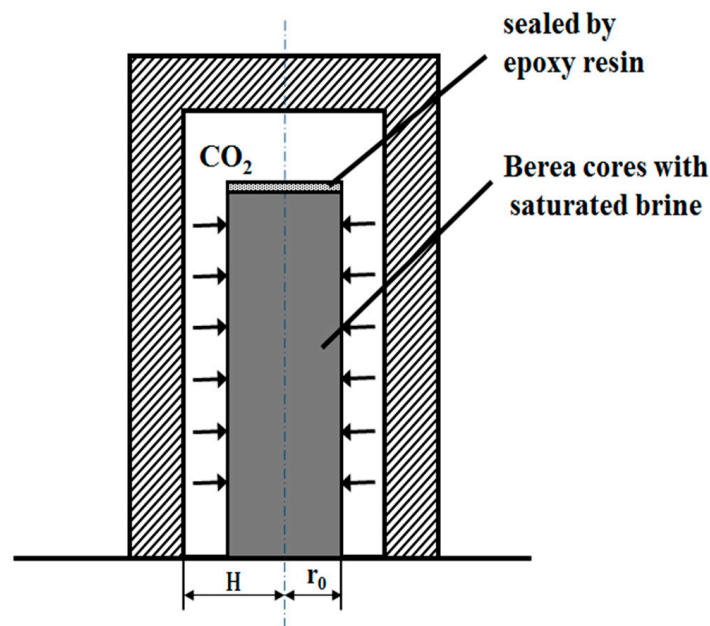


Figure 1. Schematic diagram of the CO₂/brine diffusion model.

2.2. Assumptions

The hypotheses in this study are as follows:

1. The Berea core is homogeneous, and the solution is uniformly distributed in it.
2. The swelling effect of NaCl solution is not considered in the experiments.
3. The diffusion coefficient in the core is constant.
4. Water evaporated in the experiment is negligible.

2.3. Mathematical Model

The CO₂ diffusivity in the brine-saturated homogenous core can be obtained from the continuity equation and Fick's first law, as shown in Equation (1)

$$\frac{\partial C}{\partial t} = \frac{D_{eff}}{r} \frac{\partial}{\partial r} \left(r \frac{\partial C}{\partial r} \right) \quad (1)$$

The initial conditions and the boundary conditions for this expression are

$$C = 0, 0 < r < r_0, t = 0 \quad (2)$$

$$C = C_0, r = r_0, t \geq 0 \quad (3)$$

where C is the concentration of CO_2 in the core, mol/m^3 ; r is the radius of CO_2 diffusion; $0 < r < r_0$, m ; r_0 is the core radius, m ; t is the diffusion time, $t \geq 0$, s ; D_{eff} is the CO_2 effective diffusion coefficient, m^2/s .

After conversion and simplification, the formulas for calculating the CO_2 diffusion coefficient are as follows [8,44].

$$\Delta P = k\sqrt{t} \quad (4)$$

$$D_{eff} = \frac{\pi}{4} \left(\frac{r_0 k V}{N_\infty Z R T} \right)^2 \quad (5)$$

where ΔP is the pressure variation value, Pa ; k denotes the slope; t is the diffusion time, s ; and V is the volume between the reactor and the core sample. N_∞ is the mass of CO_2 entering the core after diffusion is complete, mol . Z is the compression factor. R denotes the gas constant, $8.314 \text{ J}/(\text{mol}\cdot\text{K})$.

3. Experiment

3.1. Materials

Three kinds of Berea cores were prepared with different permeability. The porosities were 10.3%, 16.5% and 17.7%, respectively. Table 2 shows the properties of the Berea cores used in the experiment. Both ends of the Berea core were sealed to guarantee that CO_2 could diffuse into the brine-saturated core along the radial direction. Pure CO_2 was supplied by Dalian Special Gas Co. Ltd., China with a purity of 99.999%. Different aqueous concentrations of NaCl solution were prepared with pure NaCl .

Table 2. Properties of the porous media.

Number	Diameter, m	Length, m	Permeability, mD	Porosity, %
1			10	10.3
2	0.025	0.060	50	16.5
3			100	17.7

3.2. Apparatus

The experimental device diagram is shown in Figure 2. The experimental apparatus mainly includes a vacuum pump, a gas cylinder, a piston intermediate container, a pump, a diffusion cell, an oil bath, etc. The oil bath (CORID CD series, JULABO Inc., Seelbach, Germany) was used to set and maintain the temperature of the reactor with an accuracy of $\pm 0.03 \text{ K}$. The pump (D250L, Jiangsu Hai'an Oilfield Scientific Instrument Co., LTD., Jiangsu Province, China) was used to control and adjust the pressure in the reactor. The experimental pressure and temperature were measured and recorded by a pressure sensor (UNIK 5000, GE Druck Ltd., Seelbach, Germany) with an accuracy of $\pm 0.02 \text{ MPa}$ and a temperature sensor (JM618I, Jinming Instrument Co., Guangdong Province, China) with an accuracy of $\pm 0.2 \text{ K}$, respectively.

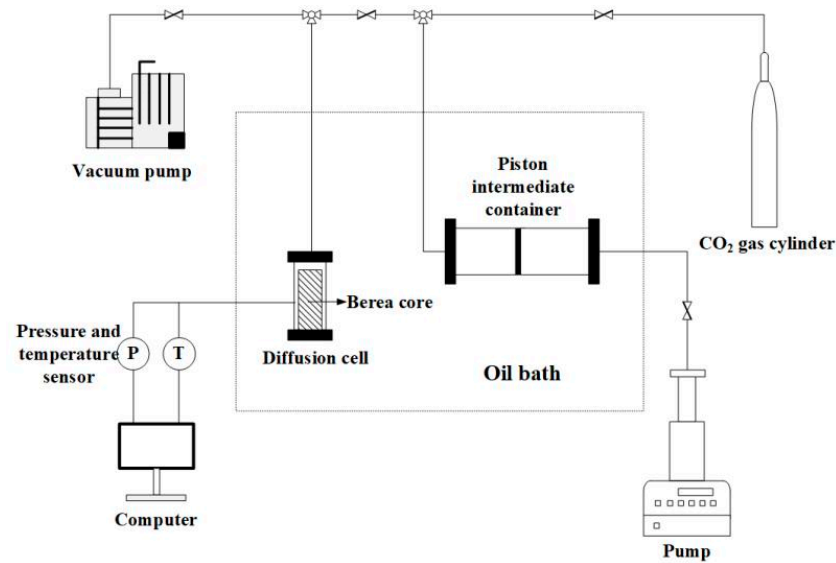


Figure 2. Schematic diagram of the CO₂/brine diffusion coefficient.

3.3. Experimental Process

The detailed steps for each diffusion coefficient test is described as follows:

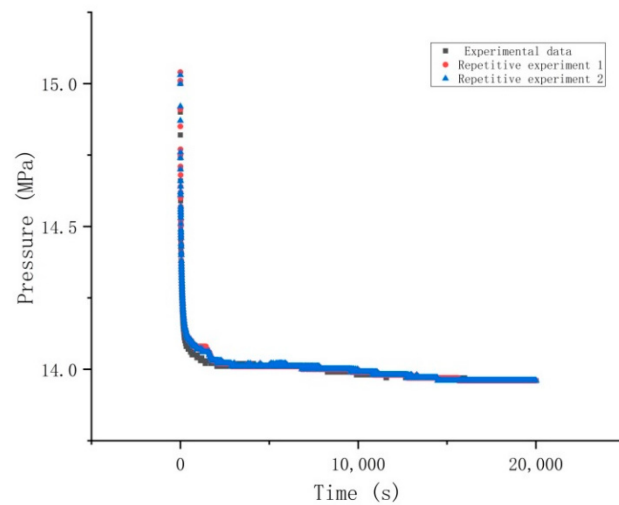
1. Different aqueous concentrations of NaCl (0.5 mol/L, 1 mol/L, 1.5 mol/L and 2 mol/L) were prepared with sodium chloride and preserved.
2. The core was completely immersed in a beaker filled with NaCl solution, vacuumed with a vacuum pump, and then allowed to stand for 24 h.
3. The pipe was purged with N₂ to ensure that there was no impurity gas in the pipe.
4. High pressure N₂ was injected into the system to ensure that there is no leakage.
5. After putting the core into the reactor, the reactor was vacuumed by a vacuum pump to guarantee that the reactor is in a vacuum state.
6. The reactor was heated to the predetermined temperature using the oil bath.
7. The CO₂ in the intermediate container was pressurized to higher than 50% of the experimental value to guarantee that the pressure in reactor could quickly reach the expected value.
8. After the intermediate container reached the expected pressure, open the valve to allow CO₂ to enter the diffusion cell. The pressure in the reactor was measured by the pressure sensor during the diffusion process and recorded in real time.
9. The diffusion process was over when the pressure in the reactor reached a steady state, and data recording was terminated. The CO₂ was released from the exhaust port, and then the Berea core and the reactor were rinsed and dried carefully.

4. Results and Discussion

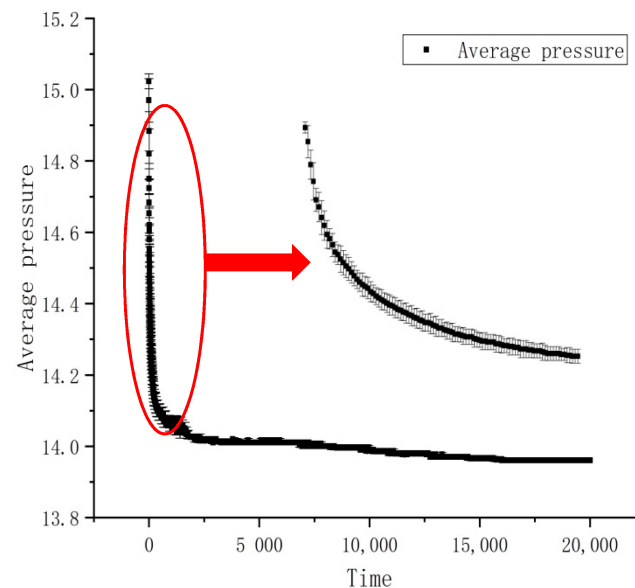
4.1. Experimental Repeatability and Reliability

To ensure the experimental reliability, repeated experiments were conducted with conditions of 15 MPa, 50 °C and 50 mD as an example, and the results are shown in Figure 3.

It can be seen from Figure 3 that at the beginning of the experiment there was little difference in the speed of the pressure drop in each group, which may be caused by an injection of high-pressure gas. Generally, the repetitive experiment maintained good consistency with the original experiment, which ensured the reliability of the experiment.



(a)



(b)

Figure 3. (a) Repeatability experiment under the conditions of 323.15 K, 15 MPa and 50 mD; (b) pressure attenuation curve with error bars and partial enlarged graph in the area between 0–200 S.

4.2. Experimental Data Summary

In this study, the control variable method was used to explore the effect of pressure, temperature, NaCl concentration and permeability on the CO₂ diffusivity in brine saturated cores. All experimental data under various conditions are shown in Table 3. The CO₂ diffusivity in the brine saturated core is on the order of 10⁻¹¹. It is noteworthy that the value of the data obtained in this study is much smaller than that in bulk brine. This is because the existence of the real core changes the diffusion path and reduces the influence of natural convection, thus greatly hindering the diffusion process. The data obtained in this experiment are also smaller than those obtained in other experiments with porous media. This is mainly caused by the following aspects. Compared with glass sand and sand cores, real cores have lower permeability, which is closer to the reservoir condition. In previous studies, CO₂ was in the gas phase. Nevertheless, CO₂ was in the supercritical state in this study, which has a larger density and viscosity compared with those in the gas phase. The diffusion process is greatly hindered, which decreases the diffusion coefficient.

Generally, the conditions in this study are closer to the actual reservoir underground. Therefore, the data from this experiment have stronger practical meaning.

Table 3. Value of the CO₂ diffusion coefficient under different conditions.

Feeds	Pressure, MPa	Temperature, K	Permeability, mD	NaCl Concentration, mol/L	Diffusion Coefficients, 10 ⁻¹¹ m ² /s
1	8.28	313.15	50	1	2.97
2	10.05	313.15	50	1	3.56
3	15.26	313.15	50	1	4.36
4	20.25	313.15	50	1	5.27
5	25.83	313.15	50	1	5.83
6	30.23	313.15	50	1	6.47
7	10.22	323.15	50	1	3.96
8	15.15	323.15	50	1	4.88
9	20.78	323.15	50	1	5.55
10	25.06	323.15	50	1	6.36
11	29.68	323.15	50	1	7.06
12	10.07	333.15	50	1	4.30
13	15.36	333.15	50	1	5.33
14	20.14	333.15	50	1	6.18
15	25.27	333.15	50	1	6.84
16	30.57	333.15	50	1	7.67
17	15	343.15	50	1	5.74
18	20.07	343.15	50	1	6.69
19	25.1	343.15	50	1	7.39
20	30.27	343.15	50	1	8.05
21	10.88	353.15	50	1	4.85
22	15.09	353.15	50	1	6.25
23	20.09	353.15	50	1	7.14
24	30.91	353.15	50	1	8.50
25	11.55	373.15	50	1	5.30
26	15.28	373.15	50	1	7.71
27	19.7	373.15	50	1	7.89
28	30.94	373.15	50	1	9.61
29	15.06	323.15	100	1	9.50
30	15	323.15	10	1	1.66
31	15.03	323.15	50	0.5	5.21
32	15.07	323.15	50	1.5	4.24
33	15.06	323.15	50	2	3.77

4.3. Effect of Temperature and Pressure on the Diffusion Coefficient of CO₂

To explore the influence of temperature, a number of experiments were carried out at 313.15 K, 323.15 K, 333.15 K, 343.15 K, 353.1 K and 373.15 K, respectively, under the same pressure. Berea cores with the NaCl concentration of 1 mol/L and the permeability of 50 mD were used in each group. The CO₂ diffusion coefficient could be obtained according to the pressure decay curve and Equation (5). The effect of temperature was shown in Figure 4.

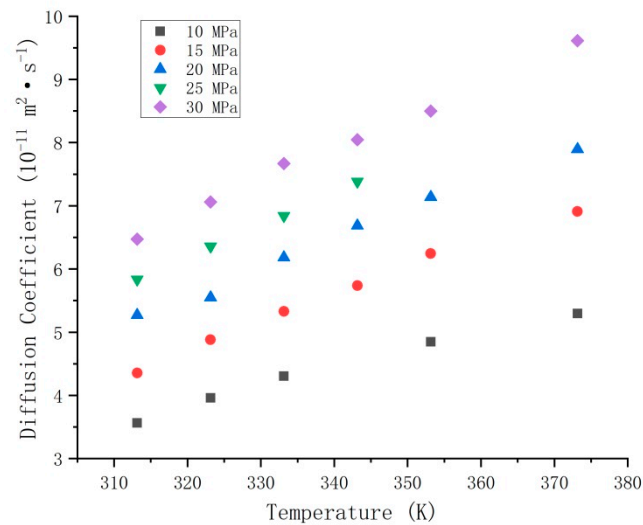


Figure 4. Diffusion coefficient of CO₂ at different temperatures.

As demonstrated in Figure 4, the diffusion coefficient increases synchronously with the temperature. This phenomenon could be explained in this way: (1) the main affecting factor in the diffusion process is the movement of thermal molecules. As the temperature increases, the movement of gas molecules becomes violent and the kinetic energy of gas molecules also increases, thereby enhancing the diffusion process. (2) As the temperature increases, the viscosity of the liquid decreases. This also accelerates the diffusion process.

In this experiment, to study the effects of pressure, experiments were conducted under the conditions of 8 MPa, 10 MPa, 15 MPa, 20 MPa, 25 MPa and 30 MPa, while the temperature and salinity remained unchanged. Each group used the Berea core with the NaCl concentration of 1 mol/L and the permeability of 50 mD. Figure 5 shows the influence of pressure on the CO₂ diffusivity. As shown from the diagram, increased pressure leads to increased diffusion coefficient. The increasing pressure leads to an increase in the supercritical CO₂ concentration in the reactor, so the diffusion rate is accelerated. However, when the experimental temperature is constant, the viscosity of CO₂ increases with increasing pressure, thereby hindering the CO₂ diffusion process. The rate at which the diffusion coefficient increases with increasing pressure is reduced.

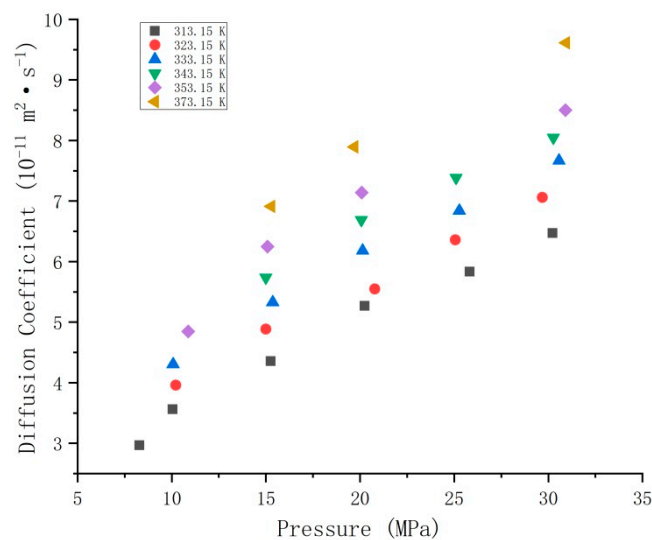


Figure 5. Diffusion coefficient of CO₂ at different pressures.

Under the condition of salinity of 1 mol/L and permeability of 50 mD, considering the influence of temperature and pressure, the empirical correlation for temperature–pressure and the CO₂ diffusion coefficient can be obtained based on the experimental data in Table 3. The empirical correlation is shown as Equation (6).

$$D = 0.19122 \times T^{0.4681} \times P^{0.51717} \quad (6)$$

Formula (7) can be obtained by non-dimensional processing of Formula (6).

$$\bar{D} = \frac{D}{D_c} = \frac{T^{0.4681} \times P^{0.51717}}{T_c^{0.4681} \times P_c^{0.51717}} = \left(\frac{T}{T_c}\right)^{0.4681} \times \left(\frac{P}{P_c}\right)^{0.51717} \quad (7)$$

where \bar{D} is the contrast diffusion coefficient $10^{-11} \text{ m}^2/\text{s}$; D is the CO₂ diffusion coefficient, $10^{-11} \text{ m}^2/\text{s}$; P is the pressure, MPa; P_c is the critical pressure, MPa; T is the temperature, °C; T_c is the critical temperature, °C.

As shown in Figure 6, the empirical correlation obtained in this paper fits well with the experimental data. The R^2 of the empirical correlation is 0.9877.

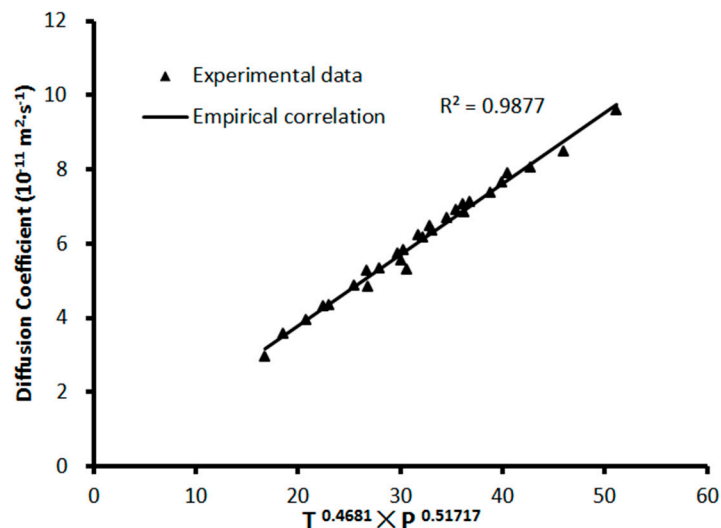


Figure 6. Comparison between empirical formula and experimental data.

4.4. Effect of NaCl Concentration on the CO₂ Diffusion Coefficient

To study the relationship between NaCl concentration and the diffusion coefficient, under the conditions of 323.15 K, 15 MPa and 50 mD, four groups of experiments with different NaCl concentrations were conducted. Figure 7 shows that the diffusion coefficient decreases as the NaCl concentration increases. The reasons for this phenomenon are as follows: the solubility of CO₂ and the viscosity of NaCl solution are related to NaCl concentration. When the NaCl concentration increases, the CO₂ solubility decreases, and the NaCl solution viscosity increases. This hinders the diffusion process of CO₂. It is instructive for us to choose the storage address. Saline aquifers with relatively low salinity are a better choice for CCS.

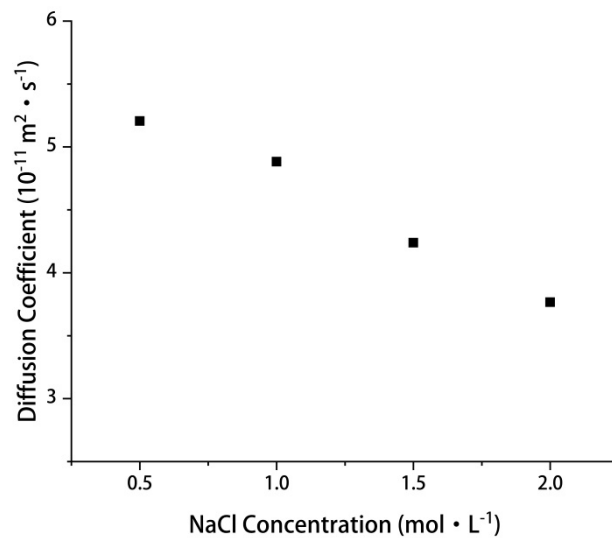


Figure 7. Diffusion coefficient of CO₂ under different NaCl concentration.

4.5. Effect of Permeability on Diffusion Coefficient

Figure 8 shows the effect of core permeability on the CO₂ diffusivity. All the experiments in the figure were performed under the conditions of a 323.15 K, 15 MPa and 1 mol/L NaCl solution. It is obvious that the increase of permeability leads to the increase of diffusion coefficient. The permeability of the core has a reciprocal relationship with the curvature of the core. The increase in permeability means a decrease in core curvature. The lower the curvature of the core, the smoother the supercritical CO₂ flow in the core, and the CO₂ diffusivity also increases.

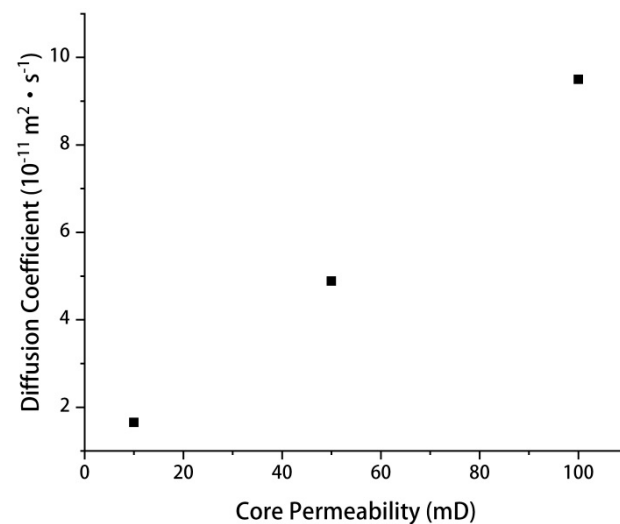


Figure 8. Diffusion coefficient of CO₂ under different permeability.

5. Conclusions

In this paper, the CO₂ diffusion coefficient in brine-saturated porous media along the radial direction was measured. It can provide a greater contact surface and makes the results more reliable. In addition, in this experiment the real core was used instead of the sand core, the pressure was up to 30 MPa and the temperature was up to 373.15 K, which simulated the underground reservoir conditions better. Overall, 33 groups of experiments were conducted at pressures ranging from 8 MPa to 30 MPa, temperatures ranging from 313.15 to 373.15 K, NaCl concentration ranging from 0.5 mol/L to 2 mol/L, and permeability ranging from 10 mD to 100 mD. The data in this paper fill the blank in the study of the CO₂ diffusion coefficient in brine under reservoir conditions.

Through experiments and result analysis, the effect of temperature, pressure, NaCl concentration and permeability on the diffusion coefficient was obtained. The CO₂ diffusion coefficient increases with increasing temperature caused by the intensification of molecular thermal motion. The increase in pressure also leads to an increase in the diffusivity. As the pressure continues to increase, the influence of pressure will decrease. In the experimental temperature and pressure range, the diffusivity decreases with increasing salinity and increases with increasing permeability. Moreover, the pressure–temperature-based empirical correlation was successfully developed to predict the CO₂ diffusion coefficient under reservoir conditions.

Author Contributions: Methodology, Z.L. and J.L.; validation, Z.L. and G.S.; formal analysis, Z.L. and L.Y.; investigation, L.Y.; resources, Y.Z.; data curation, Z.L. and L.Y.; writing—original draft preparation, Z.L.; writing—review and editing, Z.L.; supervision, Y.Z.; project administration, Y.Z.; All authors have read and agreed to the published version of the manuscript.

Funding: This research was funded by the National Natural Science Foundation of China, grant number 51976024 and the National Key Research and Development Program of China, grant number 2016YFB0600804.

Institutional Review Board Statement: Not applicable.

Informed Consent Statement: Not applicable.

Data Availability Statement: Data is contained within the article.

Conflicts of Interest: The authors declare no conflict of interest.

References

1. Zhang, M.; Mu, H.; Ning, Y.; Song, Y. Decomposition of energy-related CO₂ emission over 1991–2006 in China. *Ecol. Econ.* **2009**, *68*, 2122–2128. [[CrossRef](#)]
2. Liu, Y.; Teng, Y.; Lu, G.; Jiang, L.; Zhao, J.; Zhang, Y.; Song, Y. Experimental study on CO₂ diffusion in bulk n-decane and n-decane saturated porous media using micro-CT. *Fluid Phase Equilib.* **2016**, *417*, 212–219. [[CrossRef](#)]
3. Wang, H.; Liu, Y.; Song, Y.; Zhao, Y.; Zhao, J.; Wang, D. Fractal analysis and its impact factors on pore structure of artificial cores based on the images obtained using magnetic resonance imaging. *J. Appl. Geophys.* **2012**, *86*, 70–81. [[CrossRef](#)]
4. Yongan, Y.C.G. Accelerated mass transfer of CO₂ in reservoir brine due to density-driven natural convection at high pressures and elevated temperatures. *Ind. Eng. Chem. Res.* **2006**, *45*, 2430–2436.
5. Zheng, S.; Li, H.A.; Sun, H.; Yang, D. Determination of diffusion coefficient for alkane solvent–CO₂ Mixtures in heavy oil with consideration of swelling effect. *Ind. Eng. Chem. Res.* **2016**, *55*, 1533–1549. [[CrossRef](#)]
6. Teng, Y.; Liu, Y.; Song, Y.; Jiang, L.; Zhao, Y.; Zhou, X.; Zheng, H.; Chen, J. A study on CO₂ diffusion coefficient in n-decane saturated porous media by MRI. *Energy Procedia* **2014**, *61*, 603–606. [[CrossRef](#)]
7. Liu, S.; Zhang, Y.; Xing, W.; Jian, W.; Liu, Z.; Li, T.; Song, Y. Laboratory experiment of CO₂–CH₄ displacement and dispersion in sandpicks in enhanced gas recovery. *J. Nat. Gas Sci. Eng.* **2015**, *26*, 1585–1594. [[CrossRef](#)]
8. Li, Z.; Dong, M.; Li, S.; Dai, L. A new method for gas effective diffusion coefficient measurement in water-saturated porous rocks under high pressures. *J. Porous Med.* **2006**, *9*, 445–461. [[CrossRef](#)]
9. Zabala, D.; Nieto-Draghi, C.; de Hemptinne, J.C.; Lopez de Ramos, A.L. Diffusion coefficients in CO₂/n-alkane binary liquid mixtures by molecular simulation. *J. Phys. Chem. B* **2008**, *112*, 16610–16618. [[CrossRef](#)] [[PubMed](#)]
10. Li, S.; Li, Z.; Dong, Q. Diffusion coefficients of supercritical CO₂ in oil-saturated cores under low permeability reservoir conditions. *J. CO₂ Util.* **2016**, *14*, 47–60. [[CrossRef](#)]
11. Hangyu, W.L.S. Diffusion of carbon dioxide in tetradecane. *J. Chem. Eng. Data* **1997**, *42*, 1181–1186.
12. Wang, D.; Qiao, J.; Zhou, H.; Li, W.; Song, Y. Numerical analysis of CO₂ and water displacement in natural rock cores based on a fully heterogeneous model. *J. Hydrol. Eng.* **2016**, *21*, 04015070. [[CrossRef](#)]
13. Hu, H.; Li, X.; Fang, Z.; Wei, N.; Li, Q. Small-molecule gas sorption and diffusion in coal: Molecular simulation. *Energy* **2010**, *35*, 2939–2944. [[CrossRef](#)]
14. Li, Q.; Liu, G.; Zhang, J.; Jia, L.; Liu, H. Status and suggestion of environmental monitoring for CO₂ geological storage. *Adv. Earth Sci.* **2013**, *28*, 718–727.
15. Li, Z.; Dong, M. Experimental study of diffusive tortuosity of liquid-saturated consolidated porous media. *Ind. Eng. Chem. Res.* **2010**, *49*, 6431–6437. [[CrossRef](#)]
16. Li, Z.; Dong, M.; Shirif, E. Transient natural convection induced by gas diffusion in liquid-saturated vertical porous columns. *Ind. Eng. Chem. Res.* **2006**, *45*, 3311–3319. [[CrossRef](#)]
17. Zhao, Y.; Song, Y.; Liu, Y.; Jiang, L.; Zhu, N. Visualization of CO₂ and oil immiscible and miscible flow processes in porous media using NMR micro-imaging. *Pet. Sci.* **2011**, *8*, 183–193. [[CrossRef](#)]

18. Loulou, T.; Adhikari, B.; Lecomte, D. Estimation of concentration-dependent diffusion coefficient in drying process from the space-averaged concentration versus time with experimental data. *Chem. Eng. Sci.* **2006**, *61*, 7185–7198. [[CrossRef](#)]
19. Xu, T.; Apps, J.A.; Pruess, K. Mineral sequestration of carbon dioxide in a sandstone–shale system. *Chem. Geol.* **2005**, *217*, 295–318. [[CrossRef](#)]
20. Li, X.; Liu, Y.; Bai, B.; Fang, Z. Ranking and screening of CO₂ saline aquifer storage zones in China. *Chin. J. Rock Mech. Eng.* **2006**, *25*, 963–968.
21. Chen, C.; Zhang, N.; Li, W.; Song, Y. Water contact angle dependence with hydroxyl functional groups on silica surfaces under CO₂ sequestration conditions. *Environ. Sci. Technol.* **2015**, *49*, 14680–14687. [[CrossRef](#)] [[PubMed](#)]
22. Upreti, S.R.; Mehrotra, A.K. Experimental measurement of gas diffusivity in bitumen: Results for carbon dioxide. *Ind. Eng. Chem. Res.* **2000**, *39*, 1080–1087. [[CrossRef](#)]
23. Krooss, B.M.; Leythaeuser, D. Experimental measurements of the diffusion parameters of light hydrocarbons in water-saturated sedimentary rocks—II. Results and geochemical significance. *Org. Geochem.* **1988**, *12*, 91–108. [[CrossRef](#)]
24. Zhang, Y.; Hyndman, C.; Maini, B. Measurement of gas diffusivity in heavy oils. *J. Pet. Sci. Eng.* **2000**, *25*, 37–47. [[CrossRef](#)]
25. Riazi, M.R. A new method for experimental measurement of diffusion coefficients in reservoir fluids. *J. Pet. Sci. Eng.* **1996**, *14*, 235–250. [[CrossRef](#)]
26. Renner, T.A. Measurement and correlation of diffusion coefficients for CO₂ and rich-gas applications. *SPE Reserv. Eng.* **1988**, *3*, 517–523. [[CrossRef](#)]
27. Tang, Y.P.; Himmelblau, D.M. Effect of solute concentration on the diffusivity of carbon dioxide in water. *Chem. Eng. Sci.* **1965**, *20*, 7–14. [[CrossRef](#)]
28. Tamimi, A.; Rinker, E.B.; Sandall, O.C. Diffusion coefficients for hydrogen sulfide, carbon dioxide, and nitrous oxide in water over the temperature range 293–368 K. *J. Chem. Eng. Data* **1994**, *39*, 330–332. [[CrossRef](#)]
29. Hirai, S.; Okazaki, K.; Yazawa, H.; Ito, H.; Tabe, Y.; Hijikata, K. Measurement of CO₂ diffusion coefficient and application of lifin pressurized water. *Energy* **1997**, *22*, 363–367. [[CrossRef](#)]
30. Wang, L.S.; Lang, Z.X.; Guo, T.M. Measurement and correlation of the diffusion coefficients of carbon dioxide in liquid hydrocarbons under elevated pressures. *Fluid Phase Equilib.* **1996**, *117*, 364–372. [[CrossRef](#)]
31. Azin, R.; Mahmoudy, M.; Raad, S.M.J.; Osfouri, S. Measurement and modeling of CO₂ diffusion coefficient in Saline Aquifer at reservoir conditions. *Open Eng.* **2013**, *3*, 585–594. [[CrossRef](#)]
32. Zarghami, S.; Boukadi, F.; Al-Wahaibi, Y. Diffusion of carbon dioxide in formation water as a result of CO₂ enhanced oil recovery and CO₂ sequestration. *J. Pet. Explor. Prod. Technol.* **2016**, *7*, 161–168. [[CrossRef](#)]
33. Shi, Z.; Wen, B.; Hesse, M.; Tsotsis, T.; Jessen, K. Measurement and modeling of CO₂ mass transfer in brine at reservoir conditions. *Adv. Water Resour.* **2018**, *113*, 100–111. [[CrossRef](#)]
34. Raad, S.M.J.; Azin, R.; Osfouri, S. Measurement of CO₂ diffusivity in synthetic and saline aquifer solutions at reservoir conditions: The role of ion interactions. *Heat Mass Transf.* **2015**, *51*, 1587–1595. [[CrossRef](#)]
35. Wang, S.; Hou, J.; Liu, B.; Zhao, F.; Yuan, G.; Liu, G. The pressure-decay method for nature convection accelerated diffusion of CO₂ in Oil and water under elevated pressures. *Energy Sources Part A Recovery Util. Environ. Eff.* **2013**, *35*, 538–545. [[CrossRef](#)]
36. Zhang, W.; Wu, S.; Ren, S.; Zhang, L.; Li, J. The modeling and experimental studies on the diffusion coefficient of CO₂ in saline water. *J. CO₂ Util.* **2015**, *11*, 49–53. [[CrossRef](#)]
37. Moghaddam, R.N.; Rostami, B.; Pourafshary, P. A method for dissolution rate quantification of convection-diffusion mechanism during CO₂ storage in saline aquifers. *Spéc. Top. Rev. Porous Media Int. J.* **2013**, *4*, 13–21. [[CrossRef](#)]
38. Belgodere, C.; Dubessy, J.; Vautrin, D.; Caumon, M.-C.; Sterpenich, J.; Pironon, J.; Robert, P.; Randi, A.; Birat, J.-P. Experimental determination of CO₂ diffusion coefficient in aqueous solutions under pressure at room temperature via Raman spectroscopy: Impact of salinity (NaCl). *J. Raman Spectrosc.* **2015**, *46*, 1025–1032. [[CrossRef](#)]
39. Cadogan, S.P.; Maitland, G.C.; Trusler, J.P.M. Diffusion coefficients of CO₂ and N₂ in water at temperatures between 298.15 K and 423.15 K at pressures up to 45 MPa. *J. Chem. Eng. Data* **2014**, *59*, 519–525. [[CrossRef](#)]
40. Farajzadeh, R.; Zitha, P.L.; Bruining, J. Enhanced mass transfer of CO₂ into water: Experiment and modeling. *Ind. Eng. Chem. Res.* **2009**, *48*, 6423–6431. [[CrossRef](#)]
41. Frank, M.J.W.; Kuipers, J.A.M.; van Swaaij, W.P.M. Diffusion coefficients and viscosities of CO₂+ H₂O, CO₂+ CH₃OH, NH₃+ H₂O, and NH₃+ CH₃OH liquid mixtures. *J. Chem. Eng. Data* **1996**, *41*, 297–302. [[CrossRef](#)]
42. Lu, W.; Guo, H.; Chou, I.M.; Burruss, R.C.; Li, L. Determination of diffusion coefficients of carbon dioxide in water between 268 and 473K in a high-pressure capillary optical cell with in situ Raman spectroscopic measurements. *Geochim. Cosmochim. Acta* **2013**, *115*, 183–204. [[CrossRef](#)]
43. Sell, A.; Fadaei, H.; Kim, M.; Sinton, D. Measurement of CO₂ diffusivity for carbon sequestration: A micro-fluidic approach for reservoir-specific analysis. *Environ. Sci. Technol.* **2013**, *47*, 71–78. [[CrossRef](#)] [[PubMed](#)]
44. Lv, J.; Chi, Y.; Zhao, C.; Zhang, Y.; Mu, H. Experimental study of the supercritical CO₂ diffusion coefficient in porous media under reservoir conditions. *R. Soc. Open Sci.* **2019**, *6*, 181902. [[CrossRef](#)]